A Simplified and Fast Computing Photovoltaic Model for String Simulation under Partial Shading Condition

Razman Ayop[a*] (razman.ayop@utm.my), Chee Wei Tan[a] (cheewei@utm.my), Mohd Saiful Azimi Mahmud[a] (azimi@utm.my), S.N Syed Nasir[a] (syedazizul@fke.utm.my), Tawfik Al-Hadhrami[b] (tawfik.al-hadhrami@ntu.ac.uk), Abba Lawan Bukar[a,c] (abbalawan9@gmail.com).

[a]School of Electrical Engineering, Faculty of Engineering, Universiti Teknologi Malaysia, Malaysia.

[b]School of Science and Technology, Nottingham Trent University, Clifton Campus Clifton Lane, Nottingham.

[c]Department of Electrical and Electronics Engineering, Faculty of Engineering, University of Maiduguri, P.M.B 1069, Maiduguri, Borno State, Nigeria.

*Corresponding Author

Abstract – The photovoltaic (PV) model allows the current-voltage characteristic curves of the PV module to be represented in the simulation, which is important in the development of the PV generation system. Nevertheless, the current single PV model is not able to receive multiple irradiance and temperature input to simulate the partial shading condition. The conventional PV model with the partial shading capability requires several PV models that are connected with a bypass diode in parallel to each PV model. As a result, the computation time becomes high and the adaptability of this model is low since it requires a circuit simulation software. This paper presents an adjuster that allows a standard PV model to has partial shading capability. The proposed PV model is only applicable for the series configuration only. The single diode model with a series resistance is used to design the PV model in MATLAB/Simulink and the results have been compared and analysed with the conventional PV model. From the results, it has shown that the proposed PV model is able to be executed up to 46 times faster in computation time compared to the conventional PV model while maintaining the maximum power point error below 4%.

Keyword: partial shading, PV, bypass diode

1. Introduction

The photovoltaic (PV) module is a device that generates energy by converting the solar energy to electrical energy. The climate change crisis has made the people to move towards a cleaner energy production such as the solar PV. As a result, this technology has gain popularity throughout the years. In 2018, there has been an increment of 100 GW of global energy produced by the solar PV, which is 25% higher from the previous year [1]. This significant increase is due to the reduction of the solar PV price due to the substantial market decline in

China. The solar PV highly depends on the ambient conditions such as the irradiance and temperature. The lower the irradiance or the higher the temperature, the lower the power produced. Therefore, a suitable energy management algorithm is needed to satisfy the load demand during low irradiance and high-temperature condition [2]. The output of the solar PV is nonlinear and it requires a maximum power point tracking (MPPT) algorithm to fully utilize the capability of the solar PV [3]. Thus, the dependability on the ambient condition and nonlinear characteristic of solar PV have become research focuses to improve energy production in solar PV. Therefore, a PV model is needed to simulate the PV generation system before an actual system is implemented.

One unit of PV module consists of many PV cells while one PV array consists of many PV modules. The aforementioned PV models discussed before are able to represent a PV cell, module, or array. In an ideal condition, the PV cells, modules, or arrays receive the same irradiance. However, in practice, the irradiance received by each PV cells, modules, or arrays might be different. This condition is called partial shading and there are significant design challenges to utilize the power produced during this condition. When the irradiance is uniform, there is only one maximum power point (MPP). During partial shading, there are multiple MPPs produced. Therefore, it is harder for the MPPT algorithm to obtain global MPP, which the global MPP produces the highest power among other MPPs [3-5]. If the MPPT algorithm fails to track the global MPP, the efficiency of the PV generation system is reduced significantly.

Currently, there are two existing PV models that are commonly used in PV research, namely the single-diode and the double-diode PV model. However, these models have the limitation of inserting only one irradiance and temperature at a time. Therefore, the partial shading condition cannot be simulated directly using a single PV model. In order to achieve the partial shading capability for the PV model, several PV models need to be simulated together in the circuit simulation software to add the bypass diode [6, 7]. Although this approach is simple, the computation time is high since all the PV models need to be simulated simultaneously and it has low adaptability since the circuit simulation software is needed. Another approach is to add the output produces by the PV models [8-10]. This approach eliminates the needs of the circuit simulation software. Nevertheless, it still requires multiple PV model to be simulated together to produce an output, which has a high computational burden. The look-up table is also used in the PV model with partial shading capability [11]. The PV model is computed and saved before the simulation of the PV system begin. As a result, the computation time is reduced significantly. Nonetheless, the accuracy of the look-up table depends on the size of the data. A higher accuracy requires a larger size of data. Besides that, a different data set is needed if there are multiple irradiances or temperature settings, which further increase the size of the data. In conclusion, a partial shading PV model with a low computational burden, requires no circuit simulation software, requires a small data size, and able to change the ambient condition is needed to improve the current model.

This paper presents a single PV model with the partial shading capability with fast computation time. Only the series configuration is applicable using this method. This model is

only suitable if the bypass diode is added parallel for each PV module. The model requires no bypass diode component added parallel to the PV model. This is because the effect of adding a bypass diode parallel to the PV module is integrated within the algorithm in the proposed model. The proposed PV model is compared with the conventional PV model that is connected in series and the comparison is simulated via the circuit simulation software. Both PV models are simulated in MATLAB/Simulink simulation software and based on the single diode model with the series resistance. This PV model is chosen due to its low computation burden while maintaining acceptable accuracy. The performance of the proposed PV model is analysed based on computation time and accuracy. The benchmark is conducted by comparing the performance of the proposed PV model with the conventional PV model.

The paper starts with the design of the conventional PV model, which includes the equation of the PV model, theoretical parameters, and the effect of partial shading. The next section discusses the proposed PV model that includes the derivation and followed by the implementation of the model into the MATLAB. The last section covers the results and discussions of the proposed PV model and the comparison with the conventional PV model. The analysed performances include computation time and accuracy.

2. Photovoltaic Model

There are various PV models available such as the double diode model, single diode model, and simplified single diode model [12, 13]. Generally, the accuracy of the model increases as the complexity increases. In the case of PV models, the double diode model is suitable to be implemented for a high accuracy application [14, 15]. Nonetheless, it requires a high computational burden since there are two diode current equations considered in the calculation. The single diode model has lower computational burden compared to the double diode model [16]. However, the accuracy of the single diode model is lower compared to the double diode model.

The single diode model is simplified by removing the parallel resistance from the model [17]. The elimination process of the parallel resistance improves the computation time of the PV model but at the same time reduced the accuracy of the PV model. The ideal model does not consider the series and parallel resistances [18, 19]. It is easily solved since it does not contain any implicit equation. However, the ideal model is highly inaccurate. The single diode model with the series resistance is suitable due to its simplicity while maintaining acceptable accuracy.

2.1. Single Diode Model with Series Resistance

The circuit representation of the single diode model with the series resistance is shown in Figure 1 [17, 20]. This model is chosen as it does not have a high computational burden and it

is still able to maintain an acceptable accuracy [12]. Based on the circuit representation, the PV current, I_{pv}, is calculated using equation (1). The numerical method such as the Newton-Raphson method is used to solve equation (1) since it is an implicit equation [17].

$$I_{pv} = I_{ph} - I_s\left[exp\left(\frac{V_{pv} + I_{pv}R_s}{AV_t}\right) - 1\right] \quad (1)$$

, where I_{ph} is the photo-generating current, I_s is the saturated current, V_{pv} is the PV voltage, R_s is the series resistance, A is the ideality factor, and V_t is the thermal voltage.

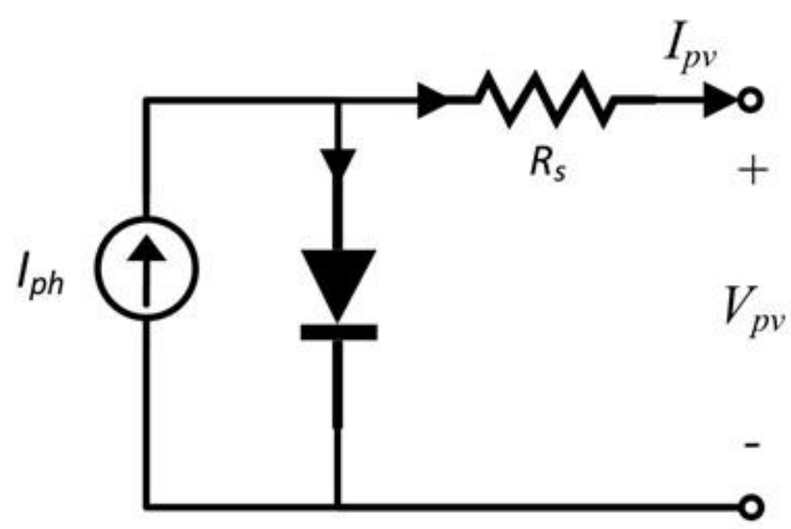

Figure 1: The circuit representation of the single diode model with series resistance.

The alternative representation of the PV model is shown in equation (2) [17]. The input of the PV model is I_{pv} and the output of the PV model is V_{pv}. This type of model is easier to compute since it is not an implicit equation. Therefore, there is no need to apply a numerical method to solve this equation.

$$V_{pv} = AV_t \times In\left[\frac{I_{ph} - I_{pv}}{I_s} + 1\right] - I_{pv}R_s \quad (2)$$

2.2. Parameters of Photovoltaic Model

The Amerisco Solar PV Module 80J-B is chosen for the simulation and the parameters are listed in Table 1 [21]. The V_t is calculated using equation (3), which this parameter changes with temperature, T [20, 22]. The I_{ph} requires the short circuit current at standard test condition (STC) (I_{sc_stc}) and temperature coefficient of short circuit current (K_{ti}) from the datasheet, which is calculated using equation (4). Parameter I_s is calculated using equation (5) and the parameters required are obtained from the manufacturer datasheet. Parameter A and R_s are adjusted manually using try and error method until the maximum power point current and voltage (I_{mp} and V_{mp}, respectively) are achieved during STC.

$$V_t = \frac{kT}{q} \quad (3)$$

$$I_{ph} = \frac{G}{G_{stc}}\left[I_{sc\_stc} + K_{ti}(T - T_{stc})\right] \quad (4)$$

$$I_s = \frac{I_{sc\_stc} + K_{ti}(T - T_{stc})}{exp\left[\frac{V_{oc\_stc} + K_{tv}(T - T_{stc})}{AV_t}\right] - 1} \quad (5)$$

, where k is the Boltzmann coefficient (1.38×10^{-23} J/K), q is the electron charge (1.6×10^{-19} C), G is the irradiance (W/m^2), G_{stc} is the irradiance at STC (1000 W/m^2), T_{stc} is the temperature at STC (298 K), V_{oc_stc} is the short circuit voltage at STC, and K_{tv} is the temperature coefficient of open circuit voltage.

Table 1: The parameters of Amerisco 80J-B (used in simulation) and Yingli YL-165 (used in experimental validation) [21, 23].

Parameter	Amerisco 80J-B	Yingli YL-165
Short Circuit Current at STC, I_{sc_stc}	2.32 A	7.90 A
Open Circuit Voltage at STC, V_{oc_stc}	44.4 V	29.0
Maximum Power Point Current, I_{mp}	2.23 A	7.20
Maximum Power Point Voltage, V_{mp}	35.8 V	23.0
Number of PV Cells in a PV Module, n_s	72	16
Temperature Coefficient of Short Circuit Current, K_{ti}	0.002 I/°C	n/a
Temperature Coefficient of Open Circuit Voltage, K_{tv}	-0.16 V/°C	n/a

2.3. Partial Shading

The partial shading occurs when a part of the module in an array receives difference G. This cause by the shows from objects like buildings and threes or the presence of dust on the PV surface. The partial shading changes the I-V and P-V characteristic curves of the PV form the standard curves, as shown in Figure 2. Figure 2(a) represents a PV array that consists of three PV module connected in series with a parallel bypass diode connected to each PV module. Region A occurs when the V_{pv} is lower than critical PV voltage 1, $V_{pv\_cri(1)}$. At this region, the resistance connected to the PV array is low. If the resistance increases, the PV array operates in Region B, which the V_{pv} is between $V_{pv\_cri(1)}$ and critical PV voltage 2, $V_{pv\_cri(2)}$. If the resistance becomes higher, the PV array operates in Region C, which the V_{pv} is more than $V_{pv\_cri(2)}$. The partial shading creates multiple MPP, as shown in Figure 2(b). The highest peak is called the global MPP and the rest of the peak is called the local peak. A good MPPT algorithm is able to detect the global MPP when the partial shading occurs.

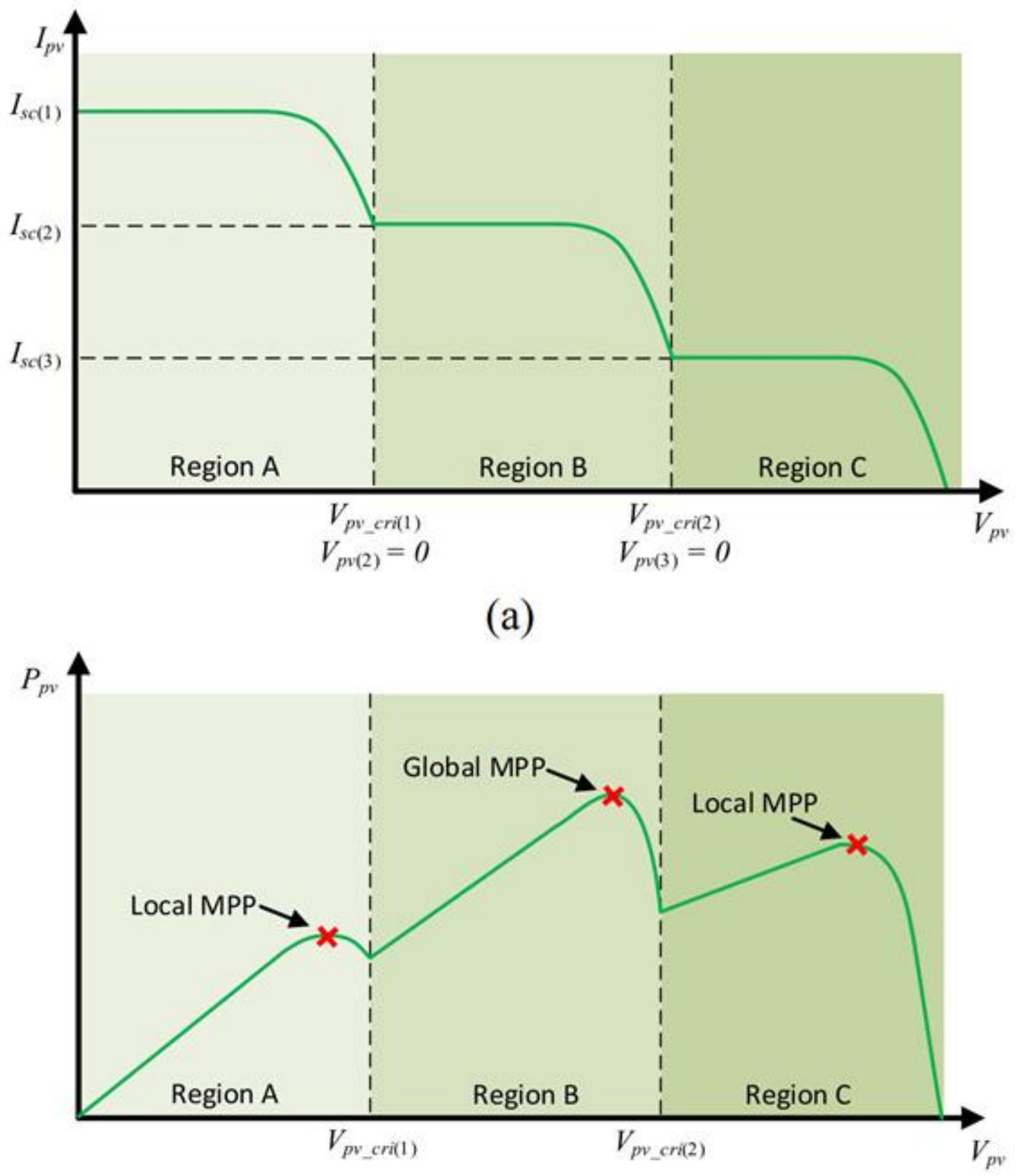

Figure 2: a) The current-voltage (I-V) and b) the corresponding power-voltage (P-V) PV characteristic curves of the three PV modules connected in series during partial shading.

The bypass diode prevents the PV array from damage during partial shading by providing an alternative path for the current. During partial shading, some of the current flow to the bypass diode, D_b. This condition normally occurs when the low load connected to a string of PV modules, which the V_{pv} is low, as shown in Figure 3. In this example, the $G_{(1)}$ is higher than $G_{(2)}$ and the $G_{(2)}$ is higher than $G_{(3)}$. Module 1, 2, and 3 receive $G_{(1)}$, $G_{(2)}$, and $G_{(3)}$, respectively. This is presented as different shade, which the higher G has a lighter shade and the lower G has a darker shade. As a result, the $I_{ph(1)}$ is higher than $I_{ph(2)}$ and the $I_{ph(2)}$ is higher than $I_{ph(3)}$. Only the PV module with the highest G has current passing through the PV diode, D_{pv}. While the other PV modules have current passing through the D_b instead of D_{pv}. For the operation in Region A shown in Figure 3(a), if the V_{pv} is measured across each PV module, only the first PV module has non-zero reading. While the second and third PV modules have zero V_{pv}.

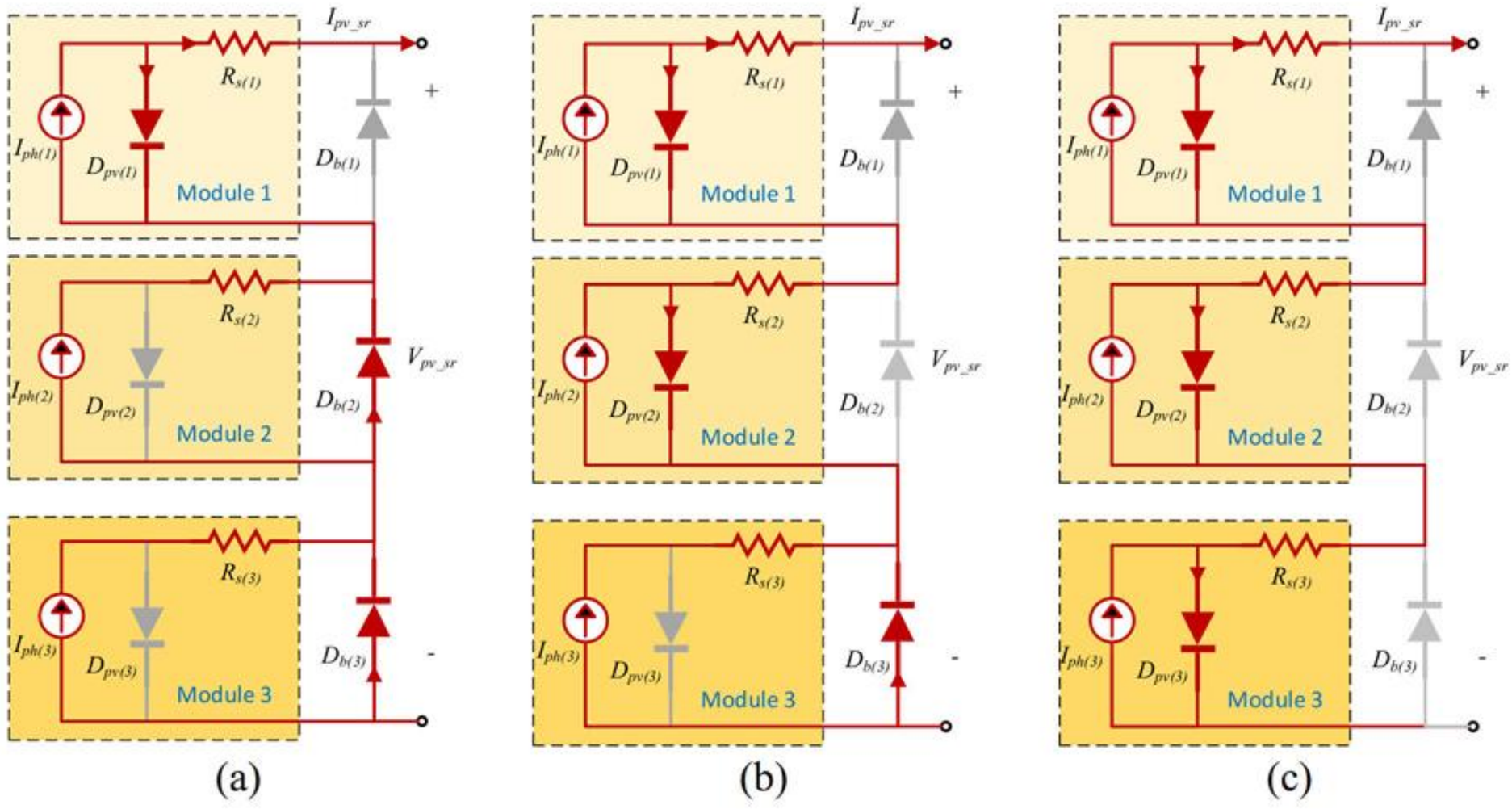

Figure 3: The operation of the three PV modules connected in series during partial shading at different region ($G_{(1)} > G_{(2)} > G_{(3)}$). a) Operation in Region A. b) Operation in Region B. c) Operation in Region C.

As the load increases, the V_{pv} increases. When the $I_{ph(2)}$ equals to the $I_{ph(1)}$ minus the current passing through $D_{pv(1)}$, the $D_{pv(2)}$ starts to operates and the voltage across $D_{b(2)}$ increases, causing the $D_{b(2)}$ to operate in reverse biased. As a result, the V_{pv} for the first and second PV modules becomes non-zero, which the PV array operates in Region B. While the V_{pv} across the third PV module maintains at zero. The load is further increased causing the V_{pv} to increase. When the $I_{ph(3)}$ equals to the $I_{ph(2)}$ minus the current passing through $D_{pv(2)}$, the $D_{pv(3)}$ starts to operates and the voltage across $D_{b(3)}$ increases, causing the $D_{b(3)}$ to operate in reverse biased. In this condition, the PV array operate in Region C. As a result, the V_{pv} for all PV modules becomes non-zero and all the D_bs operate in reverse biased.

3. Proposed Photovoltaic Model

The I-V characteristic curve and the circuit representation of the PV during partial shading is analysed. Based on the analysis, the PV model with partial shading is proposed.

3.1. Analysis of Photovoltaic Array during Partial Shading

The important parameters that need to be obtained from Figure 2(a) are the critical PV voltage, V_{pv_cri}, which include the $V_{pv\_cri(1)}$ and $V_{pv\_cri(2)}$. When the V_{pv} equals to the $V_{pv\_cri(1)}$, the I_{pv} equals to the $I_{sc(2)}$. The $I_{sc(2)}$ approximately equals to the $I_{ph(2)}$. Based on equation (2), the $V_{pv\_cri(1)}$ is derived and the result is shown in equation (6). If the difference between the $I_{sc(1)}$ and $I_{sc(2)}$ is too small, the $V_{pv\_cri(1)}$ becomes small. As a result, the I-V PV curve for $G_{(1)}$ is not shown in the overall I-V PV curve. In order for this method to work properly, the G needs to be significantly different from each other.

$$V_{pv\_cri(1)} = AV_{t(1)} \times In\left[\frac{I_{ph(1)} - I_{ph(2)}}{I_{s(1)}} + 1\right] - I_{ph(2)}R_s \quad (6)$$

The same case is observed for the $V_{pv\_cri(2)}$. When the V_{pv} equals to the $V_{pv\_cri(2)}$, the I_{pv} equals to the short circuit current 3, $I_{sc(3)}$. The $I_{sc(3)}$ approximately equals to the $I_{ph(3)}$. Based on equation (2), the $V_{pv\_cri(2)}$ is derived and shown in equation (7).

$$V_{pv\_cri(2)} = AV_{t(2)} \times In\left[\frac{I_{ph(2)} - I_{ph(3)}}{I_{s(2)}} + 1\right] - I_{ph(2)}R_s \quad (7)$$

After the observation on the I-V characteristic curve in Figure 2(a) and the derivation of equation (6) and equation (7), the equivalent circuit in Figure 3 is modified and the result of the modification is shown in Figure 4. For the operation in Region A, only Module 1 is calculated, which Module 2 and 3 are neglected, as shown in Figure 4(a). If the operation in Region 2, Module 1 becomes a voltage source and the magnitude of the voltage source is $V_{pv\_cri(1)}$, as shown in Figure 4(b). Module 2 is the only PV model calculated and Module 3 is neglected. If the operation in Region 3, Module 1 and 2 become voltage sources and the magnitude of the voltage sources are $V_{pv\_cri(1)}$ and $V_{pv\_cri(2)}$, respectively, as shown in Figure 4(c). Module 3 is the only PV model calculated.

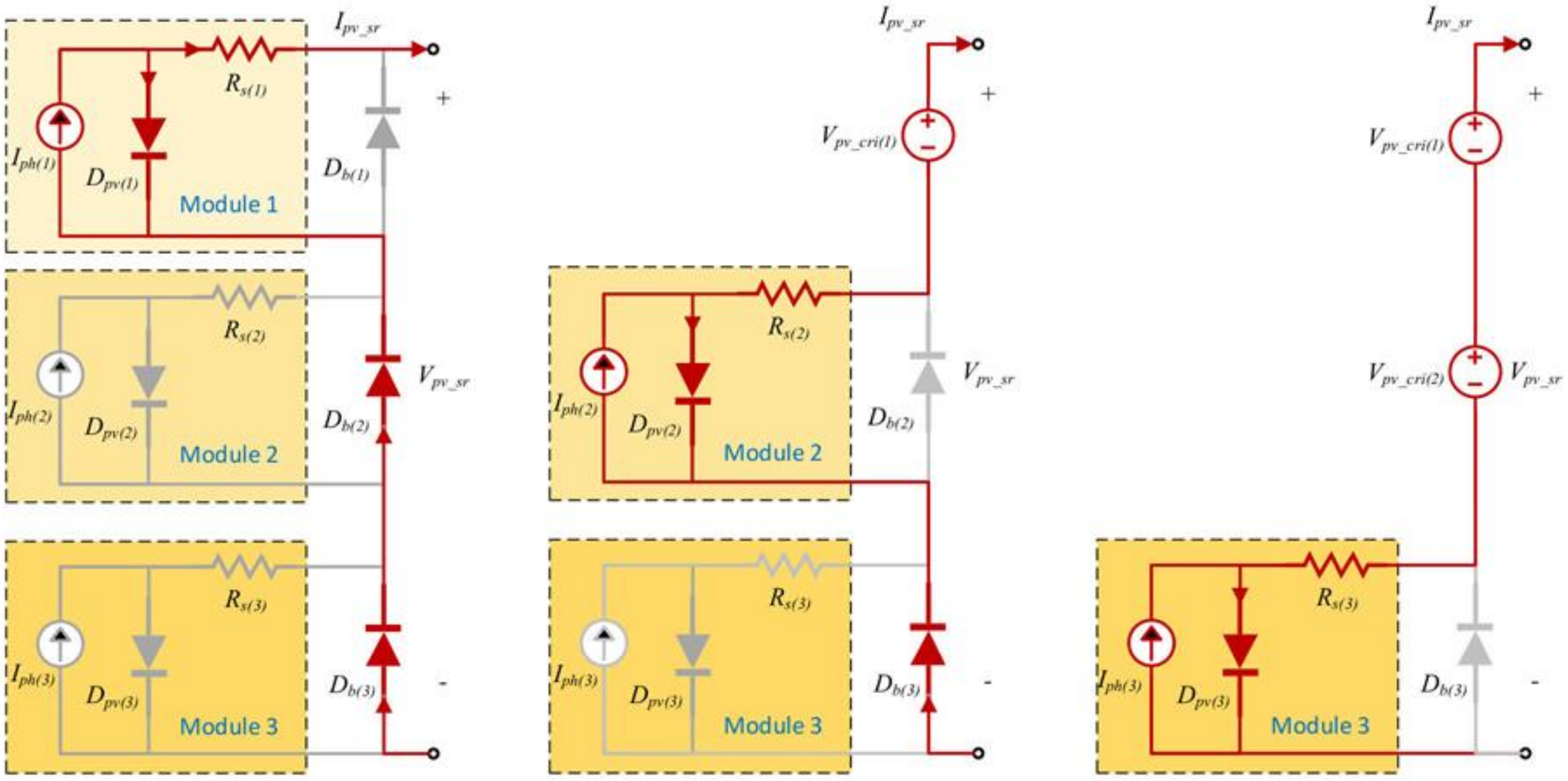

(a) (b) (c)

Figure 4: The illustration concept of the PV model during partial shading in different region ($G_{(1)} > G_{(2)} > G_{(3)}$). a) Operation in Region A. b) Operation in Region B. c) Operation in Region C.

Based on the observations on the PV array during partial shading:

- A single PV model (refer to equation (1)) capable of producing the I-V characteristic curve during partial shading by adjusting the V_{pv} that goes into the model.

- The adjustment of V_{pv} depends on the region of operation and V_{pv_cri}:
  - Region A: $V_{pv} = V_{pv\_sr}$
  - Region B: $V_{pv} = V_{pv\_sr} - V_{pv\_cri(1)}$
  - Region C: $V_{pv} = V_{pv\_sr} - V_{pv\_cri(1)} - V_{pv\_cri(2)}$

3.2. Development of the Proposed Model

The PV model with partial shading capability is proposed based on the observation on the PV array. Figure 5 shows the block diagram of the proposed PV model with partial shading capability. It consists of two parts, which are the proposed partial shading adjuster and the standard PV model. The proposed partial shading adjuster is discussed further in Figure 6. While the standard PV model is based on the equation (1). The proposed model is designed based on the PV modules connection in series with no limit on the number of PV modules connected in series, *N*. This PV model only works for simulation of the PV module with the same theoretical parameters. The proposed partial shading adjuster is derived from the single diode model with series resistance. The used of different types of conventional PV models may result in an error.

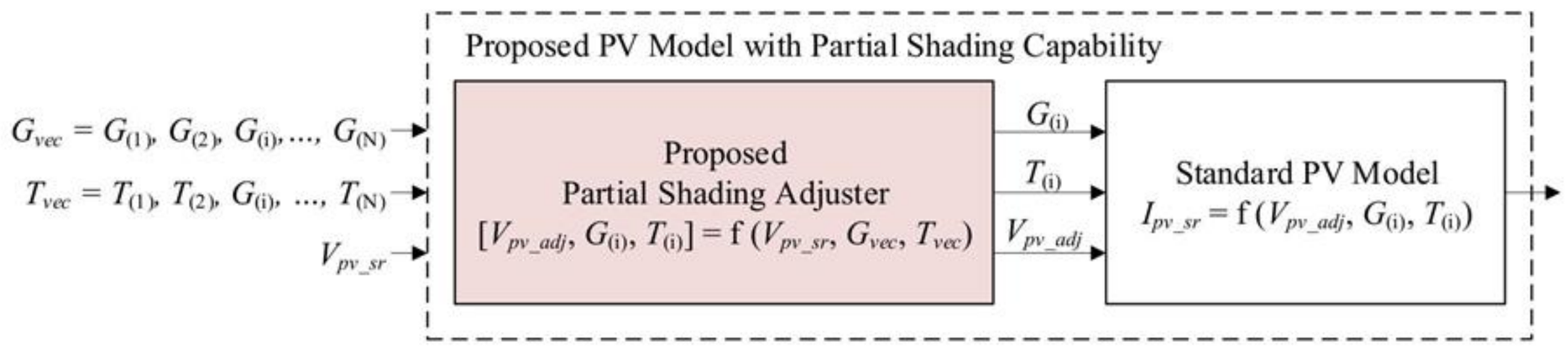

Figure 5: The block diagram of the proposed PV model with partial shading capability.

The proposed PV model requires three input and produces one output. The first input is the series PV voltage, V_{pv_sr}, which is the voltages across all the PV modules connected in series. The second and third inputs are the vector of irradiance (G_{vec}) and vector of temperature (T_{vec}). The G_{vec} consists of various G that produce the partial shading. While the T_{vec} is the corresponding T for each PV modules. The proposed partial shading adjustment analyses the V_{pv_sr}, G_{vec}, and T_{vec}, which produce the corresponding parameters that can be used by the conventional PV model (without partial shading capability). These parameters are the irradiance in i-th location in the G_{vec} (G_i), the temperature in i-th location in the T_{vec} (T_i), and the adjusted PV voltage (V_{pv_adj}). Using conventional PV model, the series PV current, I_{pv_sr}, is obtained.

The flow chart of the proposed PV model with partial shading capability is shown in Figure 6. The process started by loading the parameters of the PV module. These parameters include the I_{sc_stc}, V_{oc_stc}, n_s, K_{ti}, K_{tv}, A, and R_s. Then, the G_{vec} and T_{vec} are sorted, which the G_{vec} is sorted in descending order and T_{vec} follows G_{vec} new arrangement. If the G_{vec} is not sorted properly, the proposed partial shading adjustment will not able to be executed.

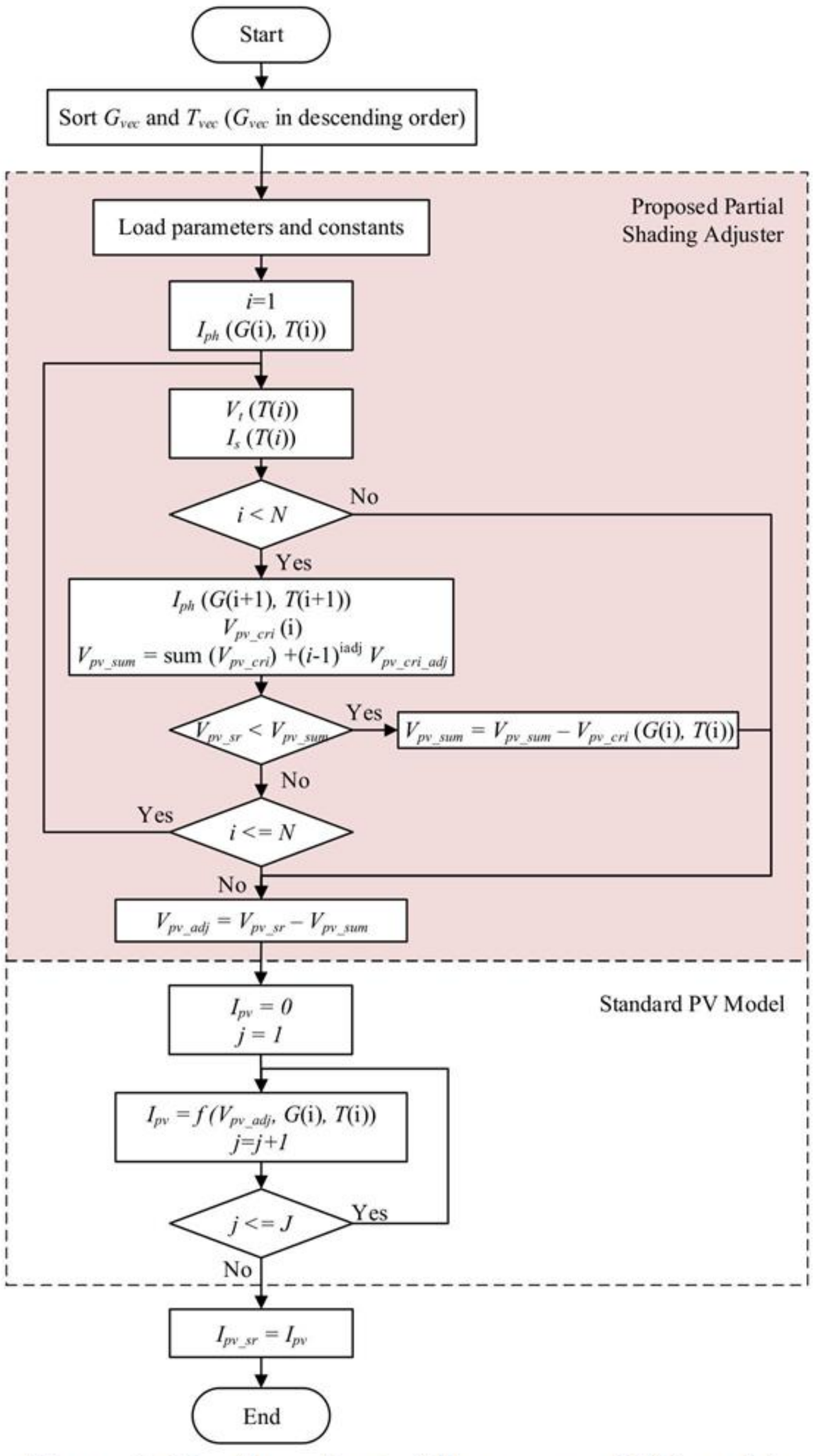

Figure 6: The flow chart of the proposed PV model.

The operation of the three PV modules connected in series similar to Figure 4 is used to describe the flow chart. The location, i, is set to 1 and the I_{ph} with $G(1)$ and $T(1)$ is calculated using equation (4). Next, the V_t(T(1)) and I_s(T(1)) are calculated using equation (3) and equation (5), respectively. Since the i is less than N (N is equal to three), the I_{ph} with $G(2)$ and $T(2)$ is calculated using equation (4). The $V_{pv\_cri}(1)$ is calculated using equation (8), which is modified from equation (6) and equation (7).

$$V_{pv\_cri}(i) = ABV_t(T(i)) - I_{ph}(G(i), T(i))R_s \tag{8}$$

$$B = In\left[\frac{I_{ph}(G(i), T(i)) - I_{ph}(G(i+1), T(i+1))}{I_s(T(i))} + 1\right]$$

The $V_{pv\_cri(1)}$ and $V_{pv\_cri(2)}$ are assumed to be constant voltage and do not change as the V_{pv} increases, as shown in Figure 4(c). This is not true since the $V_{pv\_cri(1)}$ and $V_{pv\_cri(2)}$ is changing since the current is still passing through $D_{pv(1)}$ and $D_{pv(2)}$, as shown in Figure 3(c). The higher the current passing through the D_{pv}, the higher the change of V_{pv_cri}. However, by considering the $D_{pv(1)}$, $D_{pv(2)}$ and $D_{pv(3)}$ in the PV model, the computation required is high since three currents for the diode needs to be considered. In order to overcome this problem, the V_{pv_cri} is slightly compensated based on these characteristics:

- The V_{pv_cri} is compensated as more D_{pv} is turned on.
- The compensation of the V_{pv_cri} becomes higher as more D_{pv} is turned on.
- A simple polynomial function is introduced to represent compensation.

Using the characteristics, the sum of critical PV voltage, V_{pv_sum} is derived and shown in equation (9). The parameter V_{pv_cri} is changing when the V_{pv} changes. Nonetheless, this assumption is made to reduce the processing burden. In order to reduce the error, the compensation parameters are added and these parameters are called the critical PV voltage adjustment ($V_{pv\_cri\_adj}$) and the vector adjustment, i_{adj}. The $V_{pv\_cri\_adj}$ and i_{adj} are obtained using try and error method until the I-V characteristic curve obtained from the PV model is similar to the I-V characteristic curve obtained from the conventional PV model. In this simulation, the $V_{pv\_cri\_adj}$ and i_{adj} are 3 V and 1.3, respectively.

$$V_{pv\_sum} = \sum_{i=1}^{i} [V_{pv\_cri}(i)] + (i-1)^{i_{adj}} V_{pv\_cri\_adj} \tag{9}$$

If the V_{pv_sr} is less than V_{pv_sum}, the $V_{pv\_cri}(1)$ is deducted from V_{pv_sum}. The V_{pv_adj} is calculated using equation (10) and the I_{pv_sr} is computed using the V_{pv_adj}, $G(1)$, and $T(1)$. If the V_{pv_sr} is more than V_{pv_sum}, the process of calculating the next V_{pv_cri} is started. The $V_t(2)$ and $I_s(2)$ are calculated using equation (3) and equation (5), respectively. Since the i is still less than N, the I_{ph} with $G(3)$ and $T(3)$ is calculated using the equation (4). The $V_{pv\_cri}(2)$ is calculated using equation (8) and the V_{pv_sum} is calculated using equation (9). Sum of V_{pv_cri} is the summation of $V_{pv\_cri}(1)$ and $V_{pv\_cri}(2)$. If the V_{pv_sr} is less than V_{pv_sum}, the $V_{pv\_cri}(2)$ is deducted from V_{pv_sum}. The V_{pv_adj} is calculated using equation (10) and the I_{pv_sr} is computed using the V_{pv_adj}, $G(2)$, and $T(3)$. If the V_{pv_sr} is more than V_{pv_sum}, the $V_t(3)$ and $I_s(3)$ are calculated using equation (3) and equation (5), respectively. Then, the V_{pv_adj} is calculated using equation (10) and the I_{pv_sr} is computed using the V_{pv_adj}, $G(3)$, and $T(3)$. The I_{pv_sr} is computed using the Newton-Raphson method and the number of iterations for the standard PV model, J, is 5. The J equals to 5 is chosen since it produces an acceptable error that is lower than 0.0001 A.

$$V_{pv\_adj} = V_{pv\_sr} - V_{pv\_sum} \tag{10}$$

4. Methodology

In order to analyse the performance of the proposed PV model, a comparison is made with the conventional PV model with partial shading capability. For a fair comparison, both PV models are simulated in MATLAB/Simulink software. The parameters of the PV models are based on the Amerisco 80J-B, which the parameters are listed in Table 1 [21]. While the Yingli YL-165 is used in the proposed PV model only and it is used for experimental validation [23].

4.1. Proposed PV Model

Based on the flowchart of the proposed PV model shown in Figure 6, a MATLAB function is developed. The MATLAB function is implemented in the "MATLAB Function" block, as shown in Figure 7. The MATLAB function able to receive three input (G_{vec}, T_{vec}, and V_{pv_sr}) and produce one output (I_{pv_sr}). Since the partial shading consists of various G and T, the inputs are in the form of vector. The output of the MATLAB function is connected to the "Controlled Current Source" block. The "Controlled Voltage Source" block is used to sweep the V_{pv_sr}.

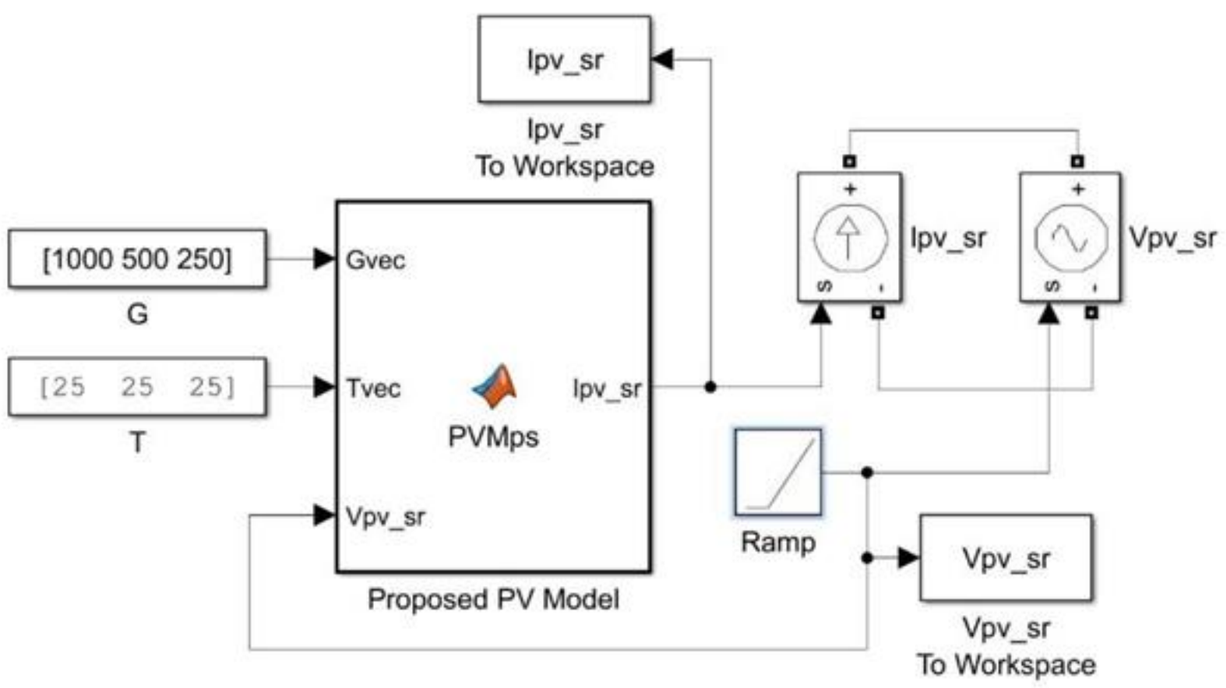

Figure 7: The simulation block of the proposed PV model.

```
function Ipv_sr = PVMps(Gvec,Tvec,Vpv_sr)
A=1.65;
Isc=2.32;
Ki=0.002;
Kv=-0.16;
Ns=72;
Rs=1;
Voc=44.4;
Vpvcriadj=3;
iadj=1.3;
k=1.38e-23;
q=1.602e-19;

Vpvsum=0;
Iph=zeros(1,length(Gvec));
Vpvcri=zeros(1,length(Gvec));
Vt=zeros(1,length(Gvec));
Is=zeros(1,length(Gvec));

%% Proposed Partial Shading Adjuster
Iph(1)=Gvec(1)/1000*(Isc+Ki*(Tvec(1)-25));
for i=1:length(Gvec)
    if i<length(Gvec)
        Iph(i+1)=Gvec(i+1)/1000*(Isc+Ki*(Tvec(i+1)-25));
    end
    Vt(i)=Ns*k*(Tvec(i)+273)/q;
    Is(i)=(Isc+Ki*(Tvec(i)-25))/(exp((Voc+Kv*(Tvec(i)-25))/(A*Vt(i)))-1);
    if i<length(Gvec)
        Vpvcri(i)=A*Vt(i)*log((Iph(i) - Iph(i+1))/Is(i) + 1) - Iph(i+1)*Rs;
    else
        break;
    end
    Vpvsum=sum(Vpvcri)+(i-1)^iadj*Vpvcriadj;
    if Vpv_sr<Vpvsum
        Vpvsum=Vpvsum-Vpvcri(i);
        break;
    end
end
Vpvsub=Vpv_sr-Vpvsum;

%% Standard PV Model
Ipv_sr=0;
for j=1:5
    Ipv_sr=Iph(i)-Is(i)*(exp((Vpvsub+Rs*Ipv_sr)/(Vt(i)*A))-1);
end
```

4.2. Conventional PV Model

The conventional method to simulate the partial shading is by simulating every single standard PV model at different G and T. These PV modules are connected using circuit simulation software such as Simulink. Then, a parallel D_b is added for each PV module. Although this method is simple to apply, the computation requirement is very high since all the PV models are simulated simultaneously. Therefore, a long processing time will be required to simulate the model. Some real-time applications such as the PV emulator is not able to implement this method due to the calculation delay which results in inaccuracy or fails to operate properly.

The conventional method to simulate the partial shading condition using the standard PV model is shown in Figure 8. Instead of using a single "MATLAB Function" block for the proposed PV model, the conventional PV model requires multiple standard PV model

connected in series in order to simulate partial shading condition. Each "MATLAB Function" block contains the standard PV model computed using the Newton-Raphson method with five iterations. The V_{pv} of each standard PV module is measured in order to calculate the I_{pv}. The output of each standard PV model is connected to individual "Controlled Current Source" block. These blocks are then connected in series together with "Controlled Voltage Source" block, which is used to sweep the V_{pv_sr}.

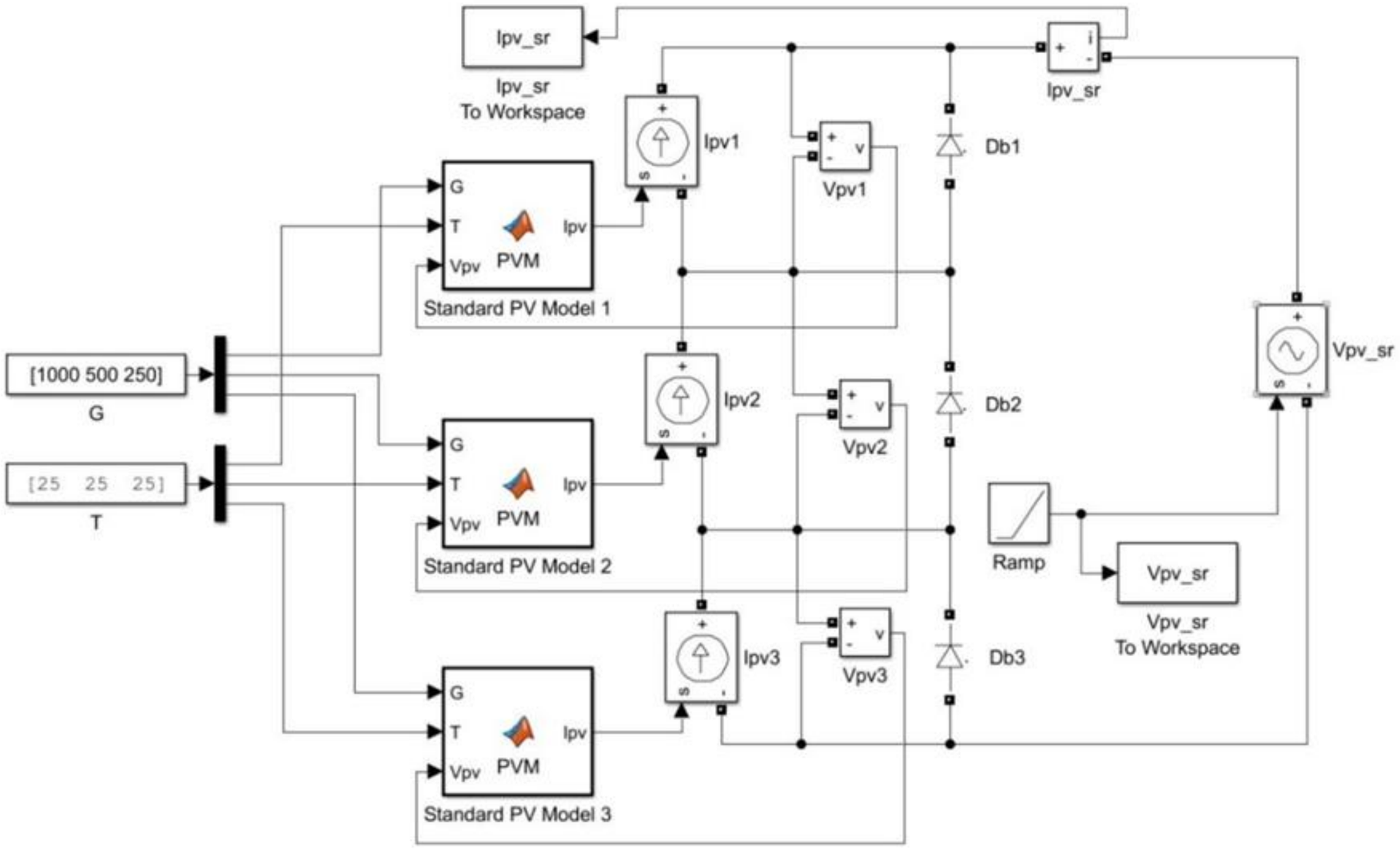

Figure 8: The simulation block of the conventional PV model.

5. Results and Discussions

The results consist of two parts, which are the simulation results and the experimental verification. Two different PV modules are used in order to analyse the performance of the proposed PV model. The Amerisco Solar PV Module 80J-B is used in the simulation results [21]. While the Yingli YL-165 is used in the experimental validation [23].

5.1. Simulation Results

The simulation results consist of two parts, which are the computation time and accuracy. The assessment has been conducted by comparing the performances between the proposed PV model with the conventional PV model. Three configurations are simulated:

- Three modules (250 W/m^2, 500 W/m^2, and 1000 W/m^2)
- Five modules (200 W/m^2 to 1000 W/m^2, with the step of 200 W/m^2)
- Ten modules (200 W/m^2 to 1000 W/m^2, with the step of 100 W/m^2)

Two performances analysis was conducted on both PV module configurations which compare the computation time and accuracy of the model for T = 25°C. Nevertheless, the proposed model is also capable of simulating various level of T.

5.1.1. Computation Time

The computation time, t_{com}, is obtained using the 'tic' and 'toc' function available in MATLAB. In order to get an accurate t_{com}, the 'tic' and 'toc' function is simulated 10 times and the average value is recorded. In addition, a similar computer system (MSI PE60 7RD) is used to simulate both proposed and conventional PV models. In the performance assessment, the faster t_{com} is preferred since it has a lower computational burden. Parameter V_{pv_sr} is chosen based on the value of N and V_{oc_stc}. For the series of three PV modules, parameter V_{pv_sr} is increased from zero to 125 V with the step input of 0.01 V. For the series of five PV modules, the V_{pv_sr} is increased from zero to 225 V with the step input of 0.01 V. For the series of ten PV modules, the V_{pv_sr} is increased from zero to 450 V with the step input of 0.01 V.

The computation time for the proposed and conventional PV model with different amount of PV modules is shown in Figure 9. For the series of three PV modules, the proposed PV model requires 0.45 s to compute while the conventional PV model requires 2.46 s to complete the model simulation. The result shows that the proposed PV model computes up to five times faster compared to the conventional PV model. For the series of five PV modules, the proposed PV model requires 0.59 s to compute while the conventional PV model requires 8.16 s to compute. The result shows that the proposed PV model computes up to 13 times faster compared to the conventional PV model. For the series of ten PV modules, the proposed PV model requires 0.99 s to compute while the conventional PV model requires 46.05 s to compute. The result shows that the proposed PV model computes up to 46 times faster compared to the conventional PV model.

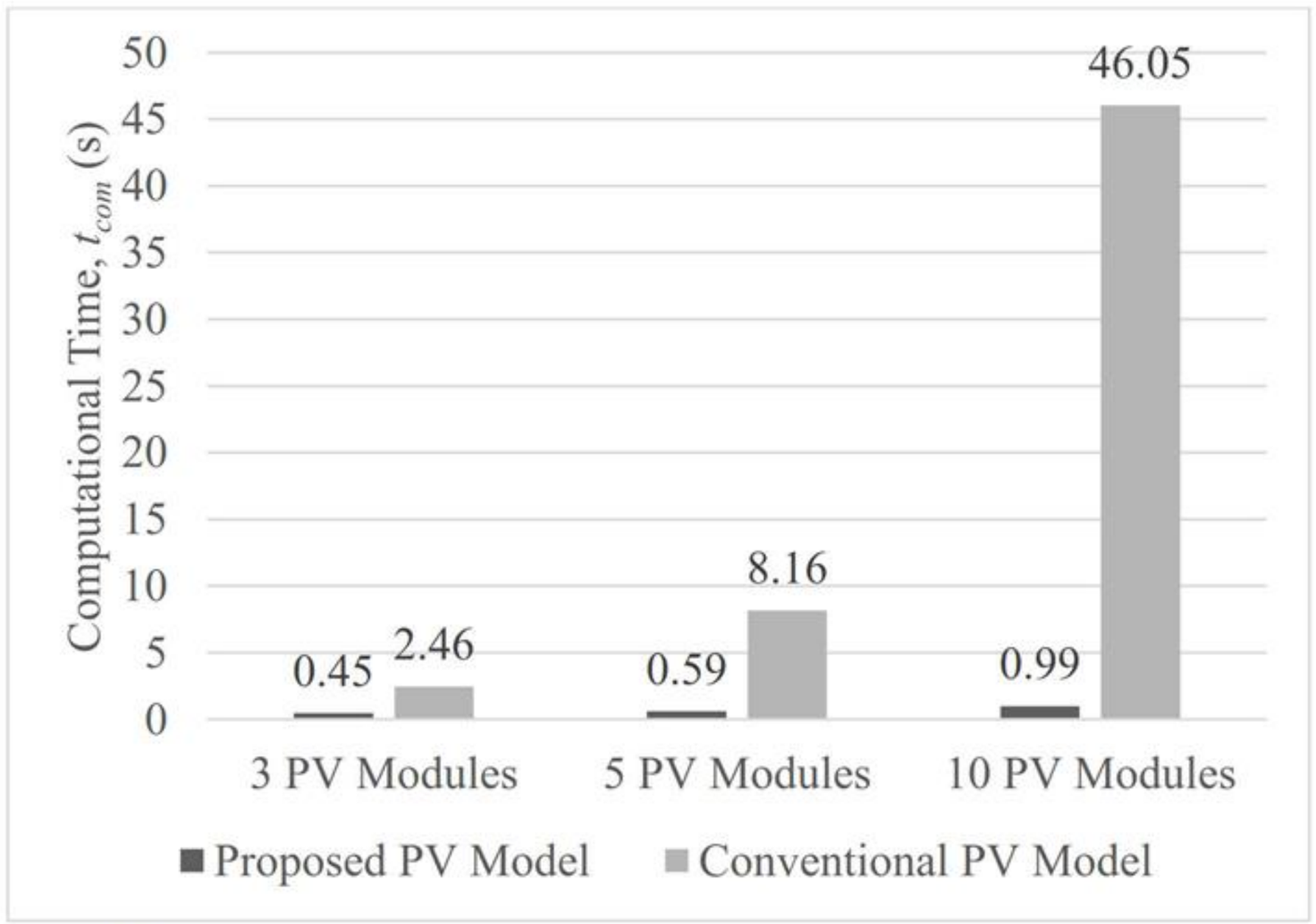

Figure 9: The computational time of the conventional and proposed PV models.

In general, the results show that the proposed PV model is faster compared to the conventional PV model, whether it is a series of three, five, or ten PV modules. The proposed PV model with the series of five PV modules requires 0.14 s (31% increases) longer time to compute compared to the series with three PV modules due to a much higher sweep voltage. The series of three PV modules is tested from zero V_{pv_sr} until 125 V. While the series of five PV modules are tested from zero V_{pv_sr} until 225 V. The similar effect is observed when series of ten PV modules is compared with the series of five PV modules, which an extra 0.4 s (68% increase) is required to sweep all the voltages.

However, the change in the computation time when the PV module increases is different for the conventional PV model. By adding an extra two PV modules, the t_{com} increases up to 5.70 s (232% increases). The conventional PV model is not suitable for a large configuration since a small increase in the number of PV modules results in a large computational burden. This effect is more severe when the series of ten PV modules is compared with the series of five PV modules, which requires an extra 37.89 s (463% increase) to compute.

The significant increase in the computation time is caused by the MATLAB/Simulink solver trying to analyse the circuit required by the conventional PV model. The increase in the number of PV modules results in a higher number of components that needs to be analysed. As a result, the computation time increases significantly as the number of PV modules increase. This is different from the proposed PV model that does not require an increase in the number of components when the number of PV modules increases.

In conclusion, the proposed PV model is significantly faster compared to the conventional PV model. The proposed PV model able to simulate the I-V characteristic of the PV modules under partial shading condition without significantly burden the processor. While the conventional PV model requires a high computational capability to simulate partial shading and the requirement significantly increases in computation time as the number of PV modules connected in series increases.

5.1.2. Accuracy

The accuracy of the proposed PV model depends on the ability of the model to produce the I-V characteristic curve similar to the conventional PV model. For a clearer result, the comparison of the power-voltage (P-V) characteristic curve is also conducted.

The results for the series of three PV modules are shown in Figure 10. Based on the results, the $V_{pv\_cri(1)}$ is found to be accurate since there is no difference between the proposed and conventional PV models at the intersection of the first and second curves. This condition is mainly due to the connection of $D_{b(2)}$ and $D_{b(3)}$ which are short-circuited, thus only one PV module operates. As a result, the calculation is simply based on one PV model. However, the accuracy of the I-V is reduced in the constant voltage region for curve two and three. During

this condition, the D_{pv} is operating and due to the simplification of the proposed PV model, only one D_{pv} is considered and the rest of D_{pv} is neglected. This situation results in a lower accuracy level in the constant voltage region. However, the computation time is found to be reduced significantly. The $V_{pv\_cri(2)}$ are slightly shifted to the right, which can be corrected by tuning the parameters $V_{pv\_cri\_adj}$ and i_{adj}. In the constant current region, the accuracy of the proposed PV model is high.

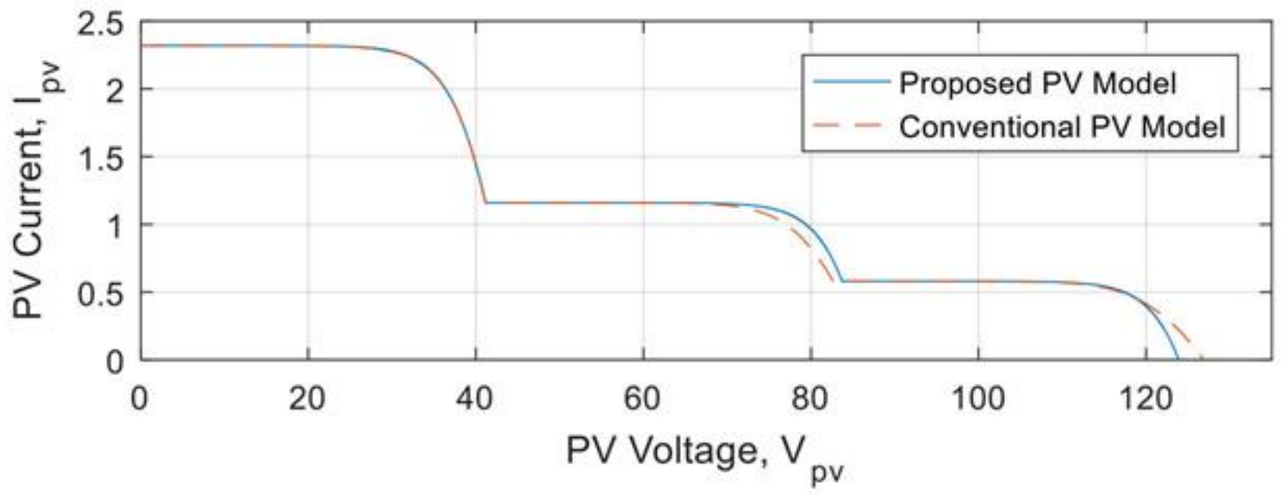

(a)

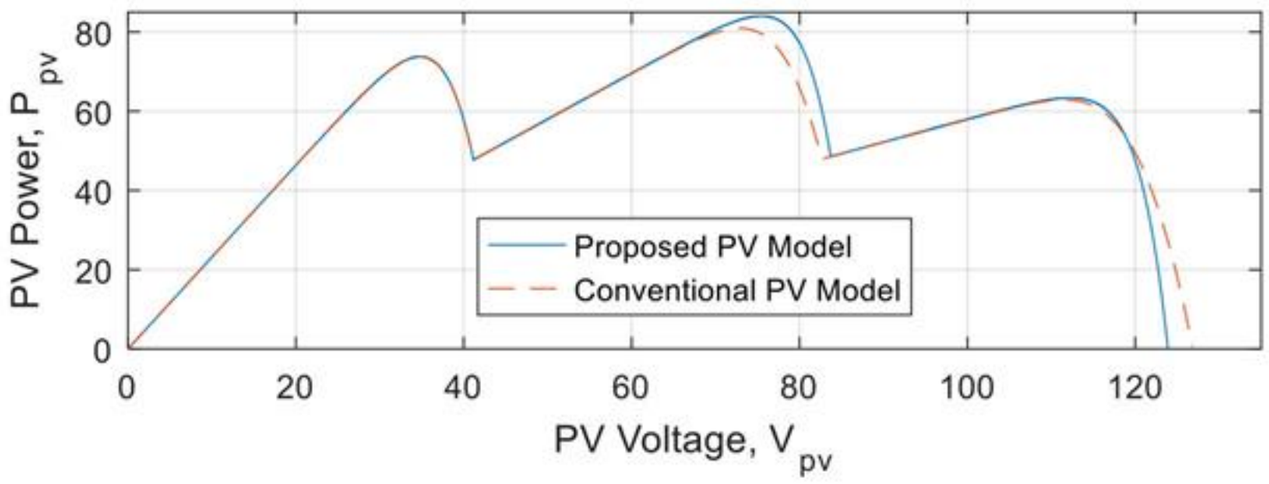

(b)

Figure 10: a) The I-V and b) the P-V characteristic curves of the conventional and proposed PV models during partial shading (250 W/m^2, 500 W/m^2, and 1000 W/m^2).

The results for the series of five PV modules are shown in Figure 11. Since some of the D_{pv} are neglected in the proposed model, the accuracy of the PV model in the constant voltage region becomes low and it becomes similar to the series of three PV modules. As a result, the MPPs are affected. This point is important, especially if the PV model is used in the MPPT application. The list of MPPs for each configuration is shown in Figure 12. The percentage power error, $e_{P\%}$, for each MPP is calculated using equation (11). The result shows that the value of $e_{P\%}$ is found between 0% to 3.9% and the value of $e_{P\%}$ is found to be zero in the first MPP. In this situation, the value of $e_{P\%}$ becomes higher as it reaches to the centre of the curve and it then decreases as the MPP becomes further away from the centre. The comparison shows that both proposed and conventional PV models have the same curve location of the global MPP. The global MPP location for the series of three, five, and ten PV modules are located at the second, fifth, and sixth curves, respectively. Since there is no difference in the location of the global MPP, the proposed PV model is accurate enough to be used in the MPPT application.

$$e_{p\%} = \frac{\left|MPP_{prop} - MPP_{conv}\right|}{MPP_{conv}} \times 100\% \tag{11}$$

where MPP_{prop} is the maximum power point of the proposed PV model and MPP_{conv} is the maximum power point of the conventional PV model.

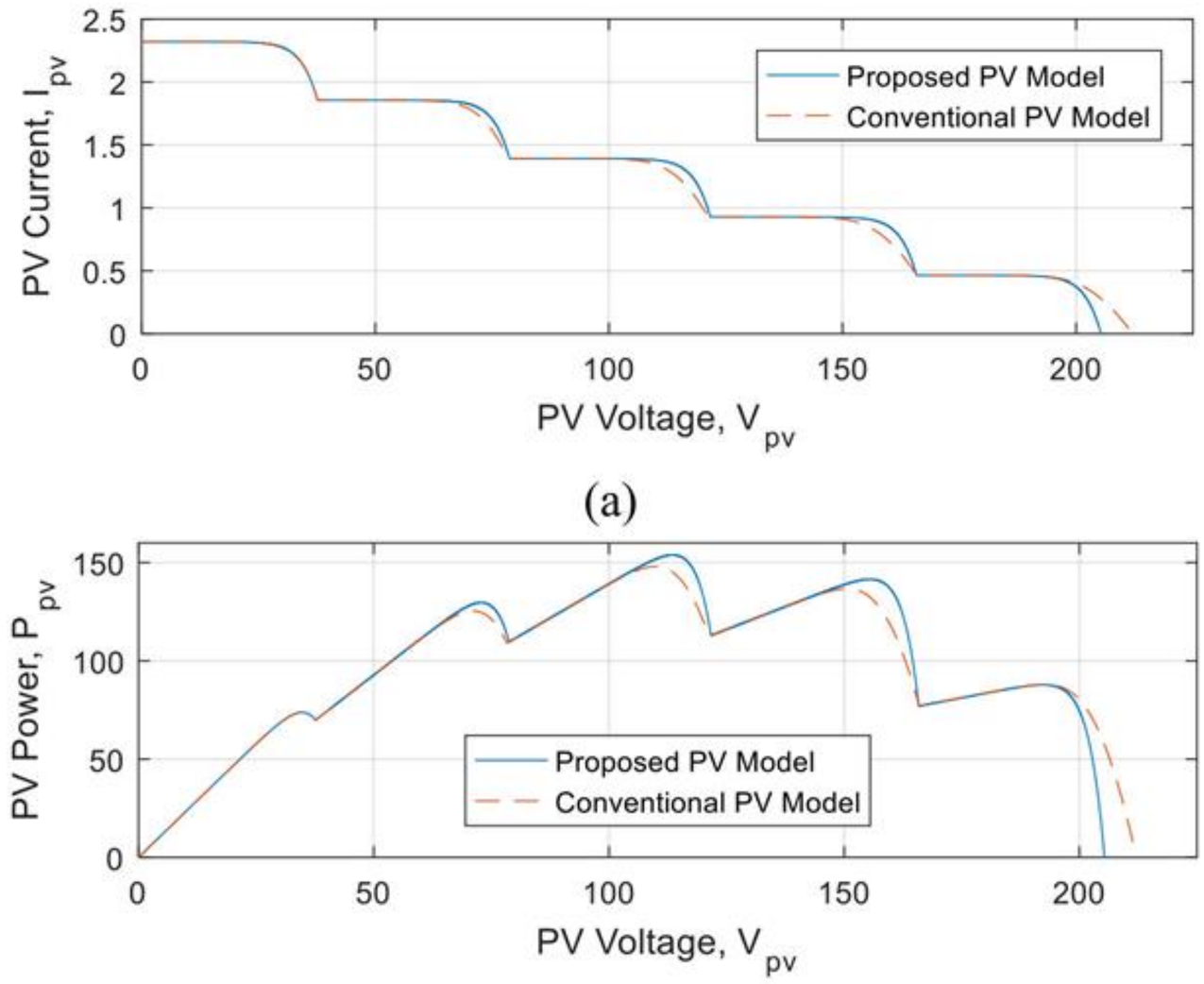

Figure 11: The a) current-voltage and b) power-voltage characteristic curves of the conventional and proposed PV models during partial shading (200 W/m^2 to 1000 W/m^2 with the step of 200 W/m^2).

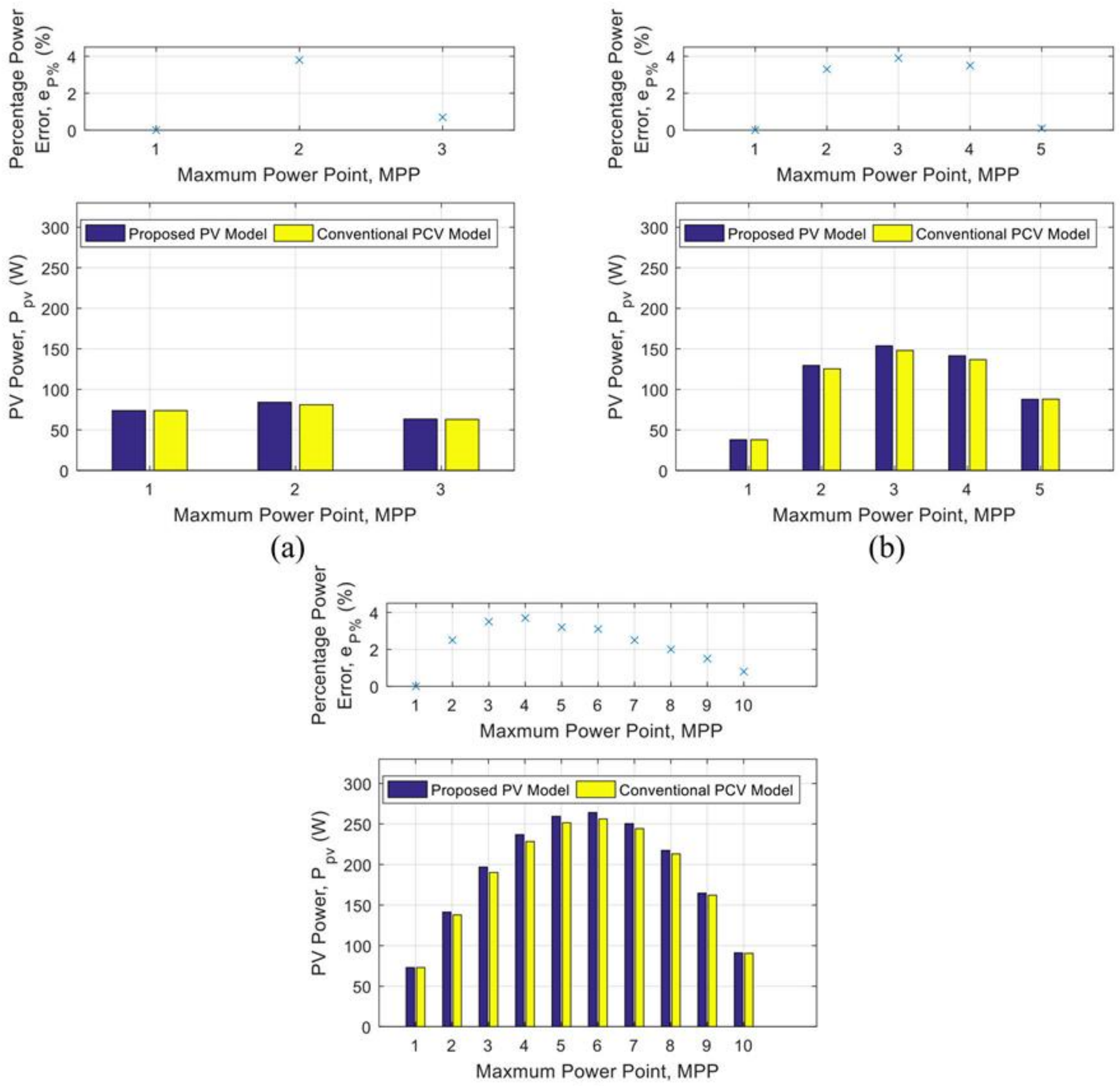

Figure 12: The MPPs for the proposed and conventional PV models and the corresponding percentage power error. a) Three modules. b) Five modules. c) Ten modules.

The results for the series of ten PV modules are shown in Figure 13. The last I-V curve in constant voltage region for every configuration shows a significant error. The proposed PV model has a steeper slope compared to the conventional PV model. As a result, the open circuit voltage of the proposed PV model is significantly lower than the conventional PV model. During this condition, only one D_{pv} operates in the proposed PV model. Nonetheless, in the actual condition, all the D_{pv} needs to be operated to produce an accurate result, which can increase the computational time.

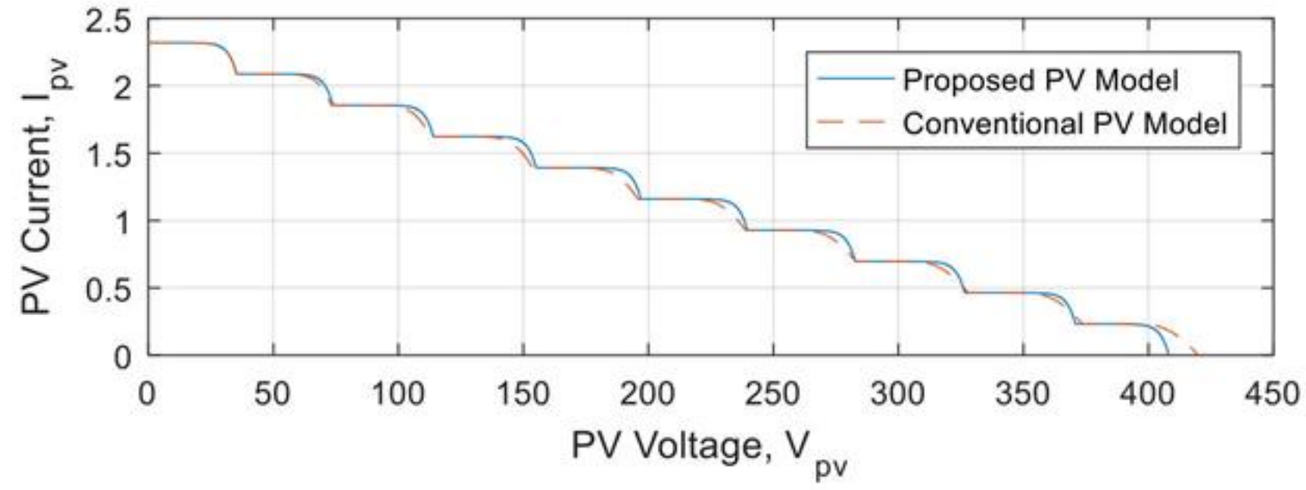

(a)

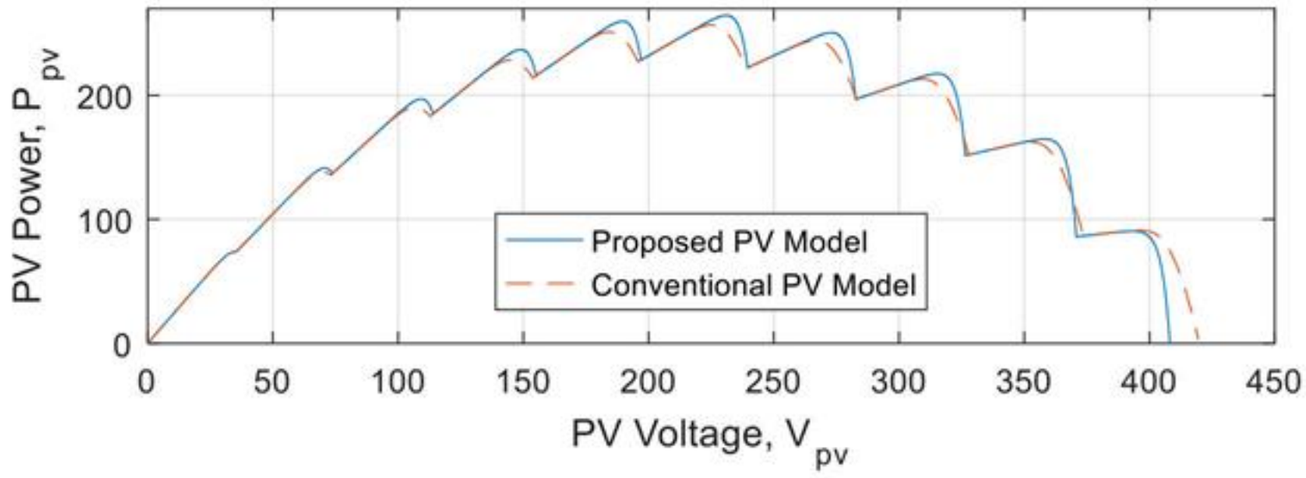

(b)

Figure 13: The a) current-voltage and b) power-voltage characteristic curves of the conventional and proposed PV models during partial shading (200 W/m^2 to 1000 W/m^2 with the step of 100 W/m^2).

Based on the results, the proposed PV model is found to be accurate compared to the conventional PV model. There is no difference observed in the constant current region. However, there is a slightly different between the proposed and conventional PV model in the constant voltage region due to the simplification process. The simplification process also produces an error at the MPP. However, this error is not affecting the location of the global MPP.

5.2. Experimental Verification

The performance of the proposed model is compared with the experimental data obtained from [23] and the results are shown in Figure 14. The overall results show that the proposed model is found to be similar to the experimental data, where there is no significant difference found in the constant current region. However, there is a slight difference in the constant voltage region as shown in Figure 14(a). By replacing MPP_{conv} with the MPP from the experiment data (MPP_{exp}) in equation (11), the $e_{p\%}$ for the first and second curves in Figure 14(b) are 2.79% and 8.37%, respectively.

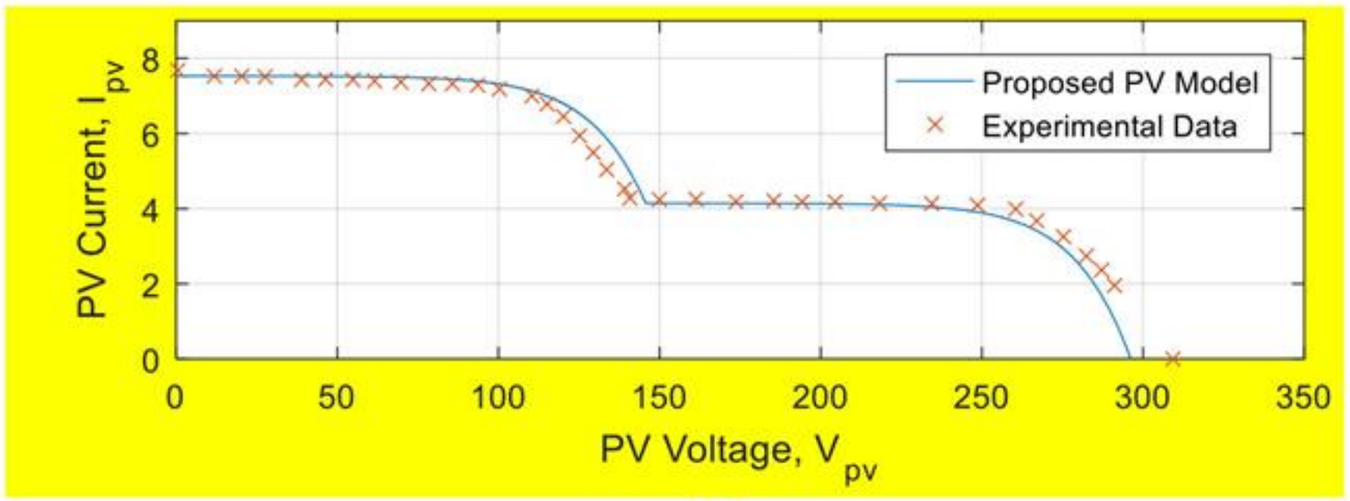

(a)

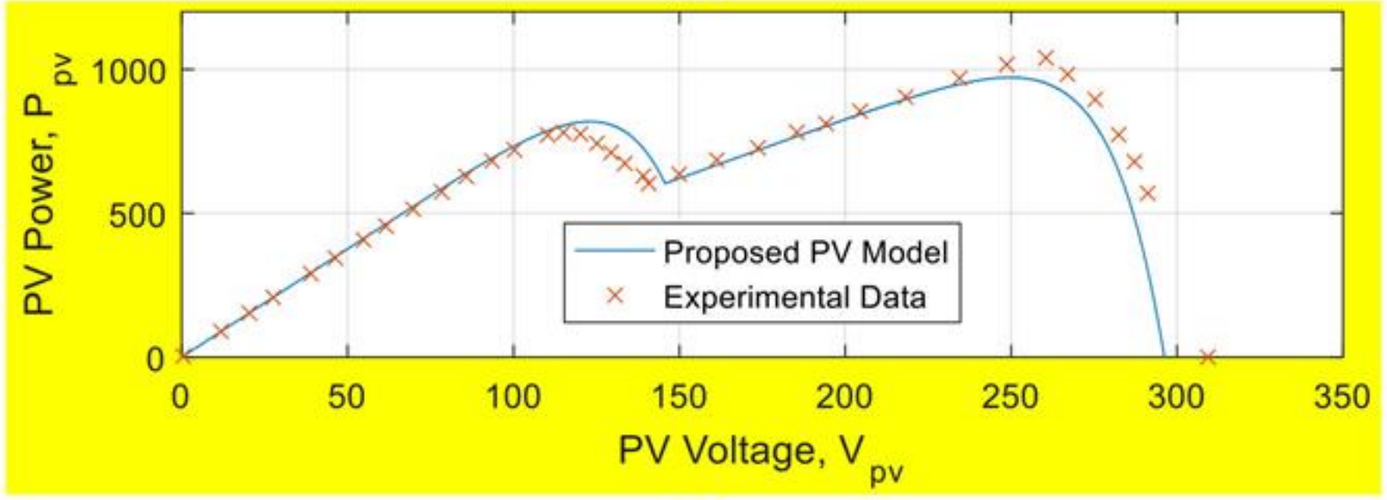

(b)

Figure 14: The a) current-voltage and b) power-voltage characteristic curves of the proposed PV model and experimental data during partial shading (550 W/m^2 and 1000 W/m^2 at 40°C).

The experimental result has shown a higher $e_{p\%}$ compared to the simulation result. By referring to the first curve, which has low V_{pv}, there is a difference between the proposed model and the experimental data in the constant voltage region. According to the simulation result, the first curve should be accurate. The difference is due to the usage of the single diode model with series resistance. In order to have higher accuracy to the experimental data, a more complex PV model such as the double diode model is needed [24]. Nonetheless, the use of the complex PV model defeats the purpose of obtaining a fast computing PV model. For the second curve, which has high V_{pv}, there is a slight difference in the constant voltage region. This difference is not only caused by the chosen PV model, but also the limitation of the proposed partial shading adjuster, which is similar to the simulation result.

6. Conclusion

The proposed PV model is introduced in order to simplify the PV generation system simulation under partial shading condition. The comparison has been made with the conventional PV model as the benchmark, which is based on circuit simulation software to connect multiple PV models. The proposed model is much simpler compared to the conventional PV model and does not require circuit simulation software to compute. When the proposed PV model is compared with the conventional PV model, the results show that there is only a small difference in the I-V and P-V characteristic curves. The difference is in the constant voltage region, which caused by the simplification of the PV diode current during partial shading condition. The simulation results show that the error at the MPP is below 4%. Even though there is a slight error in the model, the proposed PV model able to perform

significantly faster. The increases in the number of PV modules connected in series only slightly increases the computation time of the proposed PV model. The experimental results exhibit similar characteristic as compared to the simulation, with just a slight difference in the constant voltage region. As for the percentage of error at the MPP, the experimental results yield higher percentage as compared to the simulation. This is attributed to the simplified single diode model used in the proposed PV model. In summary, the proposed PV model is simpler, requires low computation time with acceptable accuracy, and there no need to implement the proposed PV model in circuit simulation software.

7. Acknowledgements

The authors would like to express gratitude to Universiti Teknologi Malaysia (UTM) for providing comprehensive library facilities and funding. Funding provided by Universiti Teknologi Malaysia Encouragement Research Grant under vote Q.J130000.2651.18J39. Lastly, thanks to colleagues who have either directly or indirectly contributed to the completion of this work.

8. References

REFRENCES:

[1] REN21, "Renewables 2019 Global Status Report (GSR)," Renewable Energy Policy Network for the 21st Century (REN21)2019.

[2] A. L. Bukar and C. W. Tan, "A Review on Stand-alone Photovoltaic-Wind Energy System with Fuel Cell: System Optimization and Energy Management Strategy," *Journal of Cleaner Production,* 2019/02/23/ 2019.

[3] R. Alik and A. Jusoh, "An enhanced P&O checking algorithm MPPT for high tracking efficiency of partially shaded PV module," *Solar Energy,* vol. 163, pp. 570-580, 2018/03/15/ 2018.

[4] R. Alik and A. Jusoh, "Modified Perturb and Observe (P&O) with checking algorithm under various solar irradiation," *Solar Energy,* vol. 148, pp. 128-139, 2017/05/15/ 2017.

[5] J. Ahmed and Z. Salam, "An Accurate Method for MPPT to Detect the Partial Shading Occurrence in a PV System," *IEEE Transactions on Industrial Informatics,* vol. 13, pp. 2151-2161, 2017.

[6] F. Belhachat and C. Larbes, "Modeling, analysis and comparison of solar photovoltaic array configurations under partial shading conditions," *Solar Energy,* vol. 120, pp. 399-418, 2015/10/01/ 2015.

[7] N. Belhaouas, M. S. A. Cheikh, P. Agathoklis, M. R. Oularbi, B. Amrouche, K. Sedraoui*, et al.*, "PV array power output maximization under partial shading using new shifted PV array arrangements," *Applied Energy,* vol. 187, pp. 326-337, 2017/02/01/ 2017.

[8] M. C. Di Piazza and G. Vitale, "Photovoltaic field emulation including dynamic and partial shadow conditions," *Applied Energy,* vol. 87, pp. 814-823, 3// 2010.

[9] R. Kadri, H. Andrei, J.-P. Gaubert, T. Ivanovici, G. Champenois, and P. Andrei, "Modeling of the photovoltaic cell circuit parameters for optimum connection model

and real-time emulator with partial shadow conditions," *Energy,* vol. 42, pp. 57-67, 6// 2012.

[10] T. D. Mai, S. De Breucker, K. Baert, and J. Driesen, "Reconfigurable emulator for photovoltaic modules under static partial shading conditions," *Solar Energy,* vol. 141, pp. 256-265, 1 January 2017.

[11] M. ALAOUI, H. MAKER, A. MOUHSEN, and H. HIHI, "Solar photovoltaic emulation under uniform irradiance and partial shading conditions using fuzzy logic control," *International Journal of Scientific and Technology Research,* vol. 8, pp. 751-757, November 2019 2019.

[12] R. Ayop and C. W. Tan, "A comprehensive review on photovoltaic emulator," *Renewable and Sustainable Energy Reviews,* vol. 80, pp. 430-452, December 2017.

[13] M. C. D. Piazza and G. Vitale, *Photovoltaic Sources: Modeling and Emulation*. Verlag, London, United Kingdom: Springer, 2013.

[14] A. C. Atoche, J. V. Castillo, J. Ortegón-Aguilar, R. Carrasco-Alvarez, J. S. Gío, and A. Colli-Menchi, "A high-accuracy photovoltaic emulator system using ARM processors," *Solar Energy,* vol. 120, pp. 389-398, 2015.

[15] K. Ishaque, Z. Salam, and H. Taheri, "Simple, fast and accurate two-diode model for photovoltaic modules," *Solar Energy Materials and Solar Cells,* vol. 95, pp. 586-594, 2// 2011.

[16] R. Ayop and C. W. Tan, "An Adaptive Controller for Photovoltaic Emulator using Artificial Neural Network," *Indonesian Journal of Electrical Engineering and Computer Science,* vol. 5, pp. 556-563, 2017.

[17] B. D. Patel and A. Rana, "A pole-placement approach for buck converter based PV array Emulator," in *2016 IEEE 1st International Conference on Power Electronics, Intelligent Control and Energy Systems (ICPEICES)*, 2016, pp. 1-5.

[18] Y. Erkaya, P. Moses, I. Flory, and S. Marsillac, "Steady-state performance optimization of a 500 kHz photovoltaic module emulator," in *2017 IEEE 44th Photovoltaic Specialist Conference (PVSC)*, 2017, pp. 1-4.

[19] B. Meyers and M. Mikofski, "Accurate Modeling of Partially Shaded PV Arrays," in *2017 IEEE 44th Photovoltaic Specialist Conference (PVSC)*, 2017, pp. 3354-3359.

[20] S. Bader, X. Ma, and B. Oelmann, "One-diode photovoltaic model parameters at indoor illumination levels – A comparison," *Solar Energy,* vol. 180, pp. 707-716, 2019/03/01/ 2019.

[21] A. Solar, "Ameresco Solar 80W (24V) Photovoltaic Modules - 80J-B (24V)," ed: Ameresco Inc., 2014.

[22] A. Rachid, F. Kerrour, R. Chenni, and H. Djeghloud, "PV emulator based buck converter using dSPACE controller," in *2016 IEEE 16th International Conference on Environment and Electrical Engineering (EEEIC)*, 2016, pp. 1-6.

[23] E. I. Batzelis, I. A. Routsolias, and S. A. Papathanassiou, "An Explicit PV String Model Based on the Lambert W Function and Simplified MPP Expressions for Operation Under Partial Shading," *IEEE Transactions on Sustainable Energy,* vol. 5, pp. 301-312, 2014.

[24] N. Belhaouas, M. A. Cheikh, A. Malek, and C. Larbes, "Matlab-Simulink of photovoltaic system based on a two-diode model simulator with shaded solar cells," *Revue RER,* vol. 16, pp. 65-73, 2013.